

University of Rhode Island

**DigitalCommons@URI**

---

Open Access Master's Theses

---

2020

# CONTROL SYSTEM FOR LOW-COST MINIATURE ISOPYCNAL FLOATS (MINIONS)' TARGETING DISTRIBUTED OBSERVATIONS OF THE OCEANIC BIOLOGICAL CARBON PUMP

Jackson Sugar

*University of Rhode Island*, [jackson.t.sugar@gmail.com](mailto:jackson.t.sugar@gmail.com)

Follow this and additional works at: <https://digitalcommons.uri.edu/theses>

---

## Recommended Citation

Sugar, Jackson, "CONTROL SYSTEM FOR LOW-COST MINIATURE ISOPYCNAL FLOATS (MINIONS)' TARGETING DISTRIBUTED OBSERVATIONS OF THE OCEANIC BIOLOGICAL CARBON PUMP" (2020). *Open Access Master's Theses*. Paper 1923.  
<https://digitalcommons.uri.edu/theses/1923>

This Thesis is brought to you for free and open access by DigitalCommons@URI. It has been accepted for inclusion in Open Access Master's Theses by an authorized administrator of DigitalCommons@URI. For more information, please contact [digitalcommons@etal.uri.edu](mailto:digitalcommons@etal.uri.edu).

CONTROL SYSTEM FOR LOW-COST MINIATURE ISOPYCNAL FLOATS  
(MINIONS) TARGETING DISTRIBUTED OBSERVATIONS OF THE  
OCEANIC BIOLOGICAL CARBON PUMP

BY  
JACKSON SUGAR

A THESIS SUBMITTED IN PARTIAL FULFILLMENT OF THE  
REQUIREMENTS FOR THE DEGREE OF  
MASTER OF SCIENCE  
IN  
OCEAN ENGINEERING

UNIVERSITY OF RHODE ISLAND

2020

MASTER OF SCIENCE THESIS  
OF  
JACKSON SUGAR

APPROVED

Thesis Committee:

Major Professor

Melissa Omand

Thomas Rossby

Brennan Phillips

Brenton DeBoef  
DEAN OF THE GRADUATE SCHOOL

UNIVERSITY OF RHODE ISLAND

2020

## ABSTRACT

The flux and attenuation of Particulate Organic Carbon (POC) export through the mid-water column has been a subject of oceanographic research for decades. The methods to sample sinking particles have remained largely unchanged, and interpretation of the data is challenged by uncertainty and sparse measurements. This need prompted our efforts to develop a standalone sensor platform for subsurface timelapse photography of accumulated particles as a proxy for carbon export, combined with simultaneous measurements of dissolved oxygen, temperature and pressure. The use of a flexible Linux single board computer with power cycling enabled the float to be: low power (for long term deployments), low cost (to be deployed en-masse), easy to operate (to be deployed opportunistically by other scientists) and flexible for future expansion and improvements.

## ACKNOWLEDGMENTS

I would like to thank the ocean engineering department for the years of guidance and freedom to explore the field of oceanography. Next, thanks to my committee members Drs. Tom Rossby and Brennan Phillips for being supportive throughout my time working on this project. Thank you to Erran Sousa for mentorship in EE and development of the Iridium solution. I'd like to thank Dr. Alyson Santoro at UCSB and Dr. Joel Llopiz at WHOI for letting me join your research cruises and the crews of the research vessels Sally Ride, Armstrong and Endeavor for the safe operations and their can-do attitude. The MINIONS has been a collaborative project, and my primary role has been the development of the control system through a research assistantship supported by NSF OTIC (1842412). The MINIONS project was additionally supported by the National Academies KECK Futures Initiative, WHOI Ocean Twilight Zone project, and NASA EXPORTS (80NSSC17K0663 and 80NSSC17K0662). Last, I need to thank my professor Dr. Melissa Omand for taking a chance on me as an undergraduate intern years

ago.

## TABLE OF CONTENTS

<b>ABSTRACT</b>	ii
<b>ACKNOWLEDGMENTS</b>	iii
<b>TABLE OF CONTENTS</b>	iv
<b>LIST OF FIGURES</b>	vi
<b>CHAPTER</b>	
<b>1 Introduction</b>	1
List of References	3
<b>2 Review of Literature</b>	4
List of References	8
<b>3 Methodology</b>	9
3.1 Description of MINION Structure	10
3.1.1 Minion Ballasting	14
3.2 Power Consumption	15
3.3 Description of the MINION Control System	16
3.3.1 MINION HAT	16
3.3.2 Real Time Clock	17
3.3.3 Accelerometer	17
3.3.4 Analog to Digital Converter	17
3.3.5 RPi Camera	18
3.3.6 MS5837-30BA Pressure Sensor	18
3.3.7 TSYS01 Temperature Sensor	19
3.3.8 Dissolved O <sub>2</sub> Sensor	19
3.3.9 Burn Wire	20
3.3.10 Iridium and GPS	20
3.3.11 Reed Switch	21
3.3.12 Batteries	22
3.4 Software	22
3.4.1 ATMEGA328P	22
3.4.2 Raspberry Pi Zero W	24
3.5 Deployment	27
3.6 Recovery	28
3.7 MINION Precursors	29
3.7.1 Surface Tethered Trap (STT) Timelapse Gel Cameras	30
3.7.2 Burn-Wire Strobe units	31
List of References	33
<b>4 Results from Research Cruises</b>	34

	<b>Page</b>
4.1 EN601 . . . . .	34
4.2 EN610 . . . . .	35
4.3 NASA EXPORTS 2018 . . . . .	36
4.4 SR1919 . . . . .	37
4.5 AR43 . . . . .	38
List of References . . . . .	39
<b>5 Conclusion</b> . . . . .	<b>41</b>
5.1 Future Development . . . . .	41
5.1.1 Acoustic tags . . . . .	41
5.1.2 LiSOCI2 Lithium Batteries . . . . .	41
5.1.3 Expendable MINION Features . . . . .	42
5.2 Conclusion . . . . .	43
List of References . . . . .	43
<b>BIBLIOGRAPHY</b> . . . . .	<b>44</b>

## LIST OF FIGURES

Figure		Page
1	Professor H. Thomas Rossby holding the largest version of a RAFOS float ever built, about 2.2 meters long. It includes a pump mechanism that forces it to float up and down to neighboring density surfaces (Rossby et al., 1994). . . . .	6
2	The Carbon Flux Explorer developed by James Bishop at UC Berkeley. A combination of the SOLO float and a custom carbon flux imaging solution. (Figure A1 of Bishop [3]) . . . . .	7
3	Solidworks render of MINION with ballast weight attached in deployed position . . . . .	10
4	Solidworks render of the MINION endcap consisting of burn wire, pressure/temperature sensor, bleed screw, strobe and camera (hydrophone and O2 sensor not included in this version) . . . . .	11
5	Close up of Blue Robotics pass-through with burnwire modification . . . . .	12
6	MINION Life Cycle from deployment to recovery. First, the Minion sinks - pulled downward by the main ballast and the excess ballast (A to B). The supplementary ballast drops and the Minion approaches an isopycnal (B to C). The Minion drifts for a predetermined duration (C to D). The main ballast drops, the Minion flips and rises to the surface (D to F). At the surface, the Minion transmits position for recovery. . . . .	13
7	MINION Ballast Tank in the Omand Lab . . . . .	15
8	The MINION HAT all in one IO expansion board provides hardware sleep, programmable IO/MOSFETS/LEDs, high accuracy timing, on board sensors and power regulation, all condensed to the form factor of the RPi Zero . . . . .	16
9	The MINION HAT is designed to be adaptable for a wide range of projects and applications. . . . .	20
10	Iridium 9602, GPS and recovery strobe assembly . . . . .	21
11	An off the shelf stack of two CR123a batteries in shrink tube . . . . .	22
12	Schematic of the ATMEGA328P flow chart. The microcontroller applies power to the RPi at 'begin'. The RPi sample cycle is described in Figure 5. . . . .	23
13	An example of the MINION RPi Config file. . . . .	25
14	MINION RPi Software Flow Chart . . . . .	26
15	MINION being lowered off the stern of the R/V Sally Ride SR1919 . . . . .	27
16	MINION recovery during SR1919 cruise . . . . .	29



Figure		Page
17	Surface Tethered Trap Gel camera examples from NASA EX-PORTS 2018 . . . . .	31
18	Internals of the self contained burn wire to be potted in an acrylic tube . . . . .	32
19	Results from Fish Tag test in the Gulf of Mexico confirming accurate localization of deployed tags. Figure reproduced from Rossby et al. 2017 . . . . .	35
20	NBST Recovery with burn wire attached and sediment trap tubes removed from SOLO float . . . . .	36
21	Surface Tethered Trap gel camera time lapse image . . . . .	36
22	Removing magnetic image surface cover during MINION deployment . . . . .	37
23	MINION pressure data from SR1919. Top panel shows the entire two records. Bottom panel shows a zoomed in view of the first 2 hours of MINION 102. . . . .	38
24	Comparison of surface drifter and MINION track after one-week with same deployment site. The dashed red track represents the surface drifter, the red dots are MINION GPS transmissions with the green X marks the final GPS call. . . . .	39
25	Single 3.6V LTC AA Battery by Xeno Energy . . . . .	42

## CHAPTER 1

### Introduction

Studying the transport of organic carbon from the ocean's surface to its depths - often referred to as carbon export or the biological carbon pump (BCP) - is crucial to understanding the global carbon cycle and building better predictions of how this cycle will be modified under a changing climate. The primary mechanism of export is through sinking particles. The "efficiency" of the BCP is dictated by the rate that the carbon is remineralized by marine bacteria in the mesopelagic and the sinking speed of the particles. The crucial measurement that integrates these two rates, is the flux of sinking organic carbon as a function of depth. Current in-situ direct observations of BCP fluxes are largely limited to analyses of the contents of particle-intercepting traps (PITs) - a proven but *costly* method limited by spatial breadth and longevity of measurements.

This thesis describes the development and application of the control system for a MINION - a MINiature IsOpycNal float, an instrument designed to supplement and mitigate the limitations of PITs traps through broad distributions of measurements. The overarching goal for these platforms is to help answer a set of research questions identified as essential by a group of scientists and engineers at a 'Pump it up' workshop held at WHOI in Sept 2017 (doi: 10.1575/1912/9328) [1]: What controls BCP export flux: physical mechanisms? biological/community structure? particle morphologies? chemical composition and density? What are the particle sinking rates? What are the associated elemental fluxes that are important for geochemical mass balances?

In order to address the questions defined during the 'Pump it up' workshop, the MINION floats were designed to be deployed in large numbers - seeding upward facing time lapse cameras and sensors throughout the upper mesopelagic ocean to obtain spatially distributed timelines of carbon export proxies and other biogeochemical parameters. The MINIONS must be water-following (Lagrangian), allowing them to image sinking marine snow that settles on an upward-facing camera (Section 3.1) while minimizing turbulence and sensor displacement relative to the water column fluctuation. They must also include basic sensors like temperature and pressure as well as an oxygen sensor (Section 3.3) that will enable calculation of mesopelagic respiration rates from the time-rate-of-change of the data. The system must be able to receive data from a ROAM acoustic tag to enable underwater geolocalization, and must be able to be deployed for durations of weeks to months. In order to achieve the broadest possible impact, the MINION control system was designed with these specific goals and mission constraints in mind:

1. Low cost for mass deployment.
2. Low power for long term (weeks to months) data collection.
3. Easy to use so that they can be deployed by other scientists opportunistically.
4. Include flexible communication options to enable the addition of more sensors.

This thesis first reviews the history of Lagrangian subsurface measurements with an emphasis on the RAFOS float - a direct precursor to this design, and the Carbon Flux Explorer that uses a similar imaging approach. Next, I provide an overview of the float, with a detailed description of the MINION control system (the major topic of this thesis). I then describe some of the systems that I developed as an

undergraduate intern in Dr. Omand's lab. That directly informed and contributed to the MINION. Lastly, I describe some of the results from research cruises that allowed me to test and demonstrate various aspects of the overall design.

### **List of References**

- [1] K. Buesseler. "Pump it Up Workshop Report." [Online]. Available: <https://hdl.handle.net/1912/9328>

## CHAPTER 2

### Review of Literature

Lagrangian observations of subsurface flows have a long history, and have typically focused on large scale dynamics. The Mid-Ocean Dynamics Experiment (MODE) in the 1970s quantified mean flows and variability in the thermocline by tracking acoustic signals from SOFAR floats (Riser and Rossby, 1983). Buoyancy-controlled versions of these floats (called 'bobbies') were used in the late 1990s during The Subduction Experiment to track subduction in the eastern North Atlantic gyre (Joyce et al. 1998). RAFOS (Ranging and Fixing Of Sound) floats, descendants of SOFAR, flipped the design (and the name) by incorporating small, low-power hydrophones as opposed to the power hungry, expensive transducers. RAFOS navigation required far fewer transducers moored at known locations for ranging. RAFOS floats incorporated a high accuracy clock allowed for long term location measurements while reducing accumulated error. The floats listen for transmissions at scheduled times and determine their location via on board processing. This location data was included in sensor data sent to shore while transmitting at the surface. This enabled float deployments in larger numbers, providing observations of mesoscale variability, and illuminating the impact of eddies and jet meanders on vertical velocity (Bower and Rossby, 1989) [1].

The basic principle of operation for the MINION is similar to its deeper, longer endurance, longer range, predecessor, the RAFOS float (Figure 1, Rossby et al., 1986) [2]. Both RAFOS and MINIONs are enclosed in glass tube housings, they measure temperature and pressure and use embedded hydrophones to records sound signals from at least two acoustic beacons. Their subsurface position is re-

constructed based on triangulation of the distances between the source and receiver estimated from arrival times (sources and floats have synchronized clocks) and the sound speed. Both styles are passively ballasted (without active buoyancy control) and designed to drift at a prescribed ambient density layer for a predetermined duration. At the end of their mission, a weight is dropped and the floats rise to the surface for data transmission. A key distinction between these two systems arises from their different data objectives. MINIONs will carry BCP-specific sensors, oxygen and a marine snow flux camera, and will target the upper water column (between the mixed layer and about 300 m depth) for durations of days to months. In contrast, RAFOS floats are designed for physical measurements, and deep deployments of up to two years. Other significant differences include physical size and the cost to produce each. MINIONs range from 16 to 22" in length, small in comparison to the typical RAFOS float at 5 to 6 feet long depending on payload. RAFOS floats typically cost \$6K whereas the MINIONs are assembled at a cost of roughly \$2K each including labor.



Figure 1: Professor H. Thomas Rossby holding the largest version of a RAFOS float ever built, about 2.2 meters long. It includes a pump mechanism that forces it to float up and down to neighboring density surfaces (Rossby et al., 1994).

More recently, the Carbon Flux Explorer (CFE) [3] developed by James Bishop at UC Berkeley combines an upward facing imaging platform (Optical Sedimentation Recorder (OSR)) and a Sounding Oceanographic Lagrangian Observer (SOLO) float [4] to resolve vertical distributions of sinking particles. The CFE's conductivity, temperature, depth (CTD) sensors and navigation is provided by the SOLO float. The external optical sensor features a baffle and funnel to consolidate descending particles onto the imaging surface. That surface is then imaged at timed intervals using three different light modes: transmitted, transmitted cross-polarized and dark field. After a pre-configured number of image samples, the sampling surface is cleared by a Seabird pump for the next cycle (Figure 2).

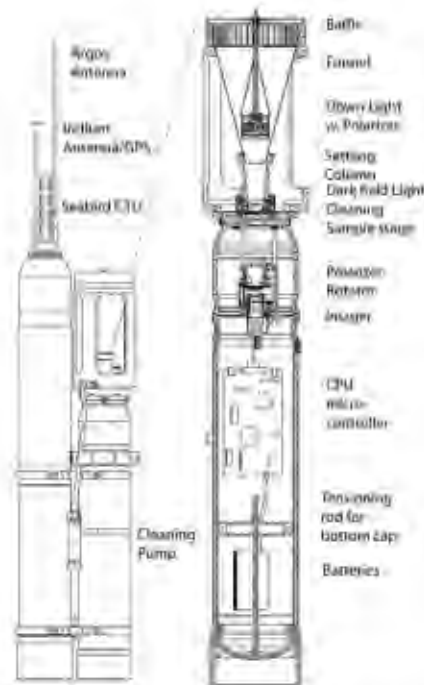


Figure 2: The Carbon Flux Explorer developed by James Bishop at UC Berkeley. A combination of the SOLO float and a custom carbon flux imaging solution. (Figure A1 of Bishop [3])

CFE deployments last days at a time with a maximum target depth of 500 meters. In a study published in 2016, both Lagrangian CFE vehicles with OSR cameras and moored OSR platforms were deployed to compare if particle size and distribution varied between sampling methods. Comparison of the resulting image data revealed that the Lagrangian CFE captured particles from 5mm to greater than a centimeter while the moored OSR images contained “only fragments of these aggregates and few particles larger than 2 mm” (Section 3.3 of [3]). This finding was attributed to turbulence generated from currents as weak as 2 cm/s at the particle baffle, that can still be much faster than the typical carbon export sinking rate of .1 cm/s and slower. These results demonstrate the advantage of Lagrangian imaging observations by mitigating surrounding fluid disturbance.

Previous studies have clearly defined the need for high volume, spatially dispersed,



long term vertical timelapse imagery of carbon flux. MINIONs combine Lagrangian sampling methods, informed by the CFE, with RAFOS positioning capabilities to add a new layer of context to observations of the oceanic biological carbon pump.

## List of References

- [1] A. S. Bower, "Potential Vorticity Balances and Horizontal Divergence along Particle Trajectories in Gulf Stream Meanders East of Cape Hatteras," *Journal of Physical Oceanography*, vol. 19, no. 11, pp. 1669–1681, 01 Nov. 1989. [Online]. Available: [https://journals.ametsoc.org/view/journals/phoe/19/11/1520-0485\\_1989\\_019\\_1669\\_pvbahd\\_2.0.co\\_2.xml](https://journals.ametsoc.org/view/journals/phoe/19/11/1520-0485_1989_019_1669_pvbahd_2.0.co_2.xml)
- [2] Rossby, Dorson, and Fontaine, "The RAFOS System," *Journal of Atmospheric and Oceanic Technology*, vol. 3, no. 4, pp. 672–679, 1986. [Online]. Available: [https://doi.org/10.1175/1520-0426\(1986\)003<0672:TRS>2.0.CO;2](https://doi.org/10.1175/1520-0426(1986)003<0672:TRS>2.0.CO;2)
- [3] J. K. B. Bishop, M. B. Fong, and T. J. Wood, "Robotic Observations of High Wintertime Carbon Export in California Coastal Waters," *Biogeosciences*, vol. 13, no. 10, pp. 3109–3129, 2016. [Online]. Available: <https://bg.copernicus.org/articles/13/3109/2016/>
- [4] D. Roemmich, J. T. Sherman, R. E. Davis, K. Grindley, M. McClune, C. J. Parker, D. N. Black, N. Zilberman, S. G. Purkey, P. J. H. Sutton, and J. Gilson, "Deep SOLO: A Full-Depth Profiling Float for the Argo Program," *Journal of Atmospheric and Oceanic Technology*, vol. 36, no. 10, pp. 1967–1981, 01 Oct. 2019. [Online]. Available: <https://journals.ametsoc.org/view/journals/atot/36/10/jtech-d-19-0066.1.xml>

## CHAPTER 3

### Methodology

The design of the MINION control system began with selection of a low cost, high resolution camera for marine snow flux imaging. The Raspberry Pi Zero W with the 8 MP camera module offers the same functionality as a full size RPi while consuming a tenth of the power due to its much less powerful processor. Since the Pi was capable of communicating with all other required sensors, it was made the primary sampling device. The Zero W variant also features on board WiFi allowing wireless access for configuring and data recovery. This is critical to avoid opening the housing after the MINION is ballasted and vacuum sealed.

A microcontroller with low power sleep functionality (ATMEGA328P) was incorporated to enable power cycling, and extend the deployment duration. This particular microcontroller is widely used in the Arduino line of education evaluation boards i.e. Arduino Nano or Pro Mini. This allowed compatibility with the Arduino IDE compiler, the most user friendly and popular compiler and programmer. Once programmed, the crystal oscillator clock on the microcontroller acts as the timekeeper while all other devices are off. During a sample cycle the controller powers the Raspberry Pi and sensors, an external real-time clock is used to append a timestamp to the measurements, and the data is saved locally at each interval. While powered, the R-Pi communicates with the microcontroller to indicate cycle completion, initiate recovery or to stand-by in the presence of the MINION Hub WiFi signal.

Hardware such as the Raspberry Pi and Arduino compatible microcontrollers

meant for the classroom setting are often well supported by manufacturers and benefit from a large user base. The intersection of flexibility, low cost, and accessibility satisfied our criteria for the MINION control system.

### 3.1 Description of MINION Structure

The MINION housing consists of three parts: a Pyrex glass tube, acrylic endcap, and a 3D printed ‘birdcage’ ballast offset bracket.

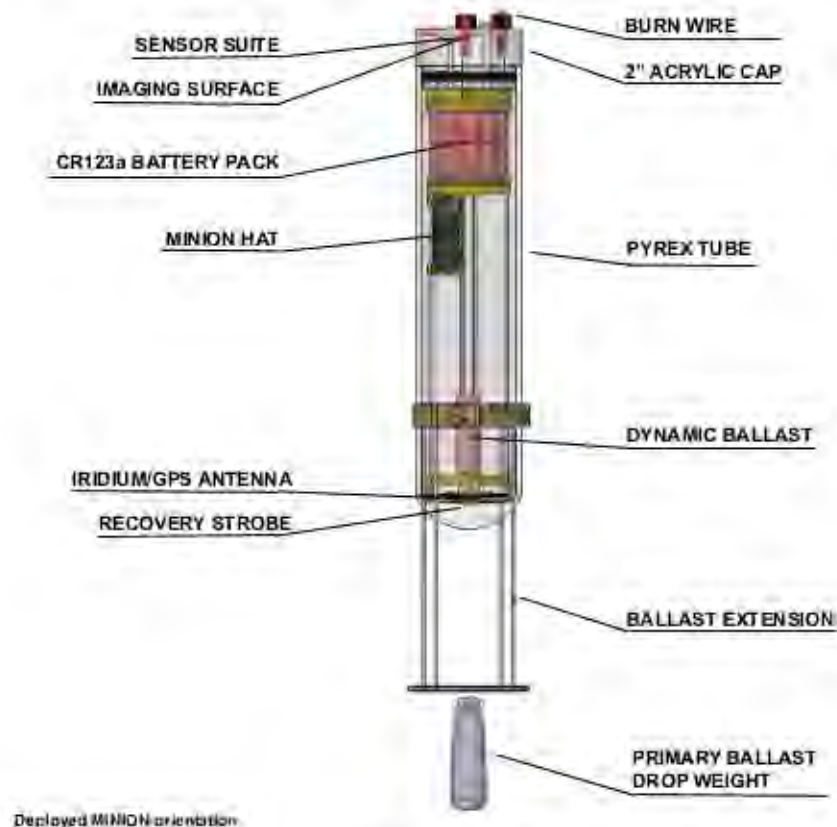


Figure 3: Solidworks render of MINION with ballast weight attached in deployed position

Following the RAFOS float design, Pyrex glass was chosen as the main external housing since it is largely incompressible, has a low coefficient of thermal expansion, and is environmentally friendly if the float is not recovered. Tubes with a 90mm O.D. and 5mm wall thickness were purchased from Wale Apparatus, cut, rounded

closed (one end only) and annealed at Finkenbeiner Inc. in Waltham, MA (Figure 3). A ‘birdcage’, is fixed to the outside of the glass with a 3D-printed resin clamp, aluminum posts and a resin halo. The halo has a series of holes at the center to allow the user to select one to pass the ballast filament through and compensate for small tilts that arises from radial asymmetries in the center of mass. Overall, the cage serves two purposes: 1) It provides a bale that may be used for recovery, and 2) shifts the MINION’s center of mass by increasing the moment applied by the ballast weight, enhancing stability while the float is deployed.

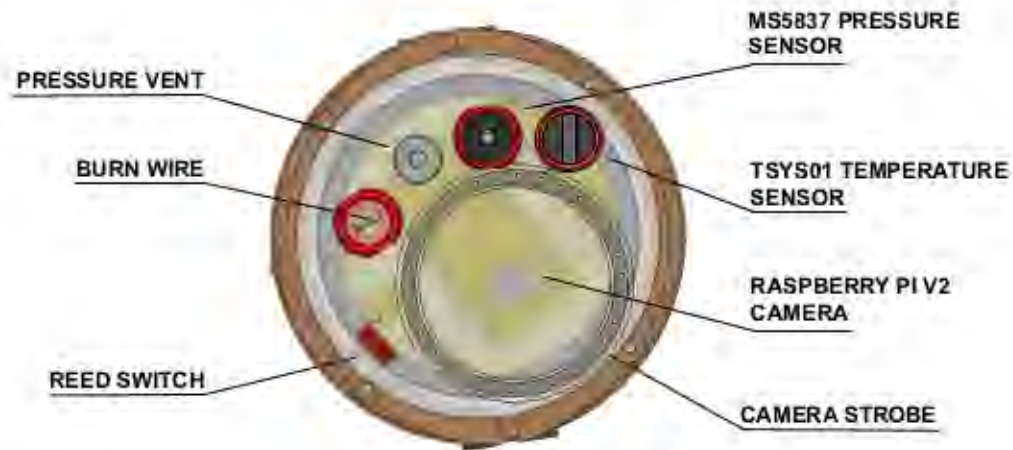


Figure 4: Solidworks render of the MINION endcap consisting of burn wire, pressure/temperature sensor, bleed screw, strobe and camera (hydrophone and O2 sensor not included in this version)

A thick, cast acrylic sheet was selected for the single end-cap, because it is sufficiently optically clear and also easy to machine (Figure 4). The thickness (1.5”) was found to be the optimal distance between the focal plane and flux camera, providing a  $\sim 10 \text{ cm}^2$  imaged area. Thus, the camera and internals can be mounted directly onto this inner face. Fully ballasted, the MINION weighs 2 kg.





Figure 5: Close up of Blue Robotics pass-through with burnwire modification

A 60 mm diameter LED ring (‘angel eyes’ car headlights) is recessed and epoxied into the endcap for illuminating the particles on the imaged surface. A pressure bleed screw consisting of a simple nylon shoulder screw and o-ring creates a boss seal on a tapered inner surface. A custom vacuum tool (based on a device for Slocum gliders by Teledyne Webb Research) is used to pull a vacuum inside the float before deployment. The vacuum reduces the humidity and prevents condensation on the lens, and also holds the endcap tightly in place. An aluminum pass-through (Blue Robotics), is used to construct a burn-wire (Figure 5). An Inconel loop anode is epoxied into the pass-through opening. The anodizing is sanded off of the outer surface, and a ground wire is fixed on the inside, press fit between an aluminum tube and the inner surface of the shaft of the pass-through. These expendable burn wire units can then be readily replaced by unthreading from the endcap.



Figure 6: MINION Life Cycle from deployment to recovery. First, the Minion sinks - pulled downward by the main ballast and the excess ballast (A to B). The supplementary ballast drops and the Minion approaches an isopycnal (B to C). The Minion drifts for a predetermined duration (C to D). The main ballast drops, the Minion flips and rises to the surface (D to F). At the surface, the Minion transmits position for recovery.

Before deployment, the Minions are ballasted to target a particular isopycnal within the main thermocline. The Minions are deployed from a research vessel descending to their target isopycnal typically within 30 min (Figure 6, A to C). The Minion then drifts for a predefined duration (typically 24 hours to weeks), taking photographs and measurements between sleep cycles (Figure 6, C to D). The flux camera consists of an upward-facing charged coupled device (CCD) camera sensor with a macro lens is mounted below the transparent end-cap. During deployment, sinking particles accumulate on this surface and are photographed, providing information on the amount and composition of these carbon-rich particles.

At the end of the mission, a ballast weight is released, the orientation of the centers of mass and buoyancy reverse, and the Minion flips over (Figure 6, E).

At the surface, the upper few inches of the domed part of the housing with a strobe and embedded Iridium and GPS antenna emerges and begins transmitting for recovery and/or data transmission(Figure 6, F).

### 3.1.1 Minion Ballasting

In order to properly ballast each MINION, a custom tank (Figure 7) was constructed in the Watkins Lab by Professor Omand and Ben Hodges (WHOI). At 4 feet deep, 7 inch inner diameter and inch thick walls, the chamber can be pressurized up to 500 psi with the tank filled with fresh or saltwater from a holding reservoir (allowing the water to reach a stable room temperature and to re-use saltwater).

A 'chain method' is employed to accurately determine the amount of added weight needed for each Minion to hit their desired isopycnal target. A metal chain of known, uniform density is hung from the float (additional ballast is needed) such that the vehicle is suspended in the water column with part of the chain resting on the bottom of the tank. Before pressurizing, the links suspended in water are counted. The added ballast should be sufficient to allow for an initial descent (as trapped air and other compressible parts are squeezed, typically over the first 50 psi). After this small descent, the Minion become less compressible than water and it will rise gradually as the pressure is increased. By counting the number of linkages in the chain at various pressure levels (ideally encompassing the target pressure) the density and compressibility of the float can be accurately determined to within about 0.05 g/ml.





Figure 7: MINION Ballast Tank in the Omand Lab

### 3.2 Power Consumption

With the 84 Wh capacity battery stack, if the RPi was continuously powered, the batteries would last less than 2 days. In order to achieve timelapse mission durations on the order of weeks to months, we required a method to minimize sensor power consumption between each timelapse sample. In both the STT cameras and Burn Wire Strobe units (see Section 5.1 on MINION precursors), we take advantage of the ATMEGA328P's idle sleep function to reduce power consumption to  $\mu$ Amps and keep time while the control system remains asleep between samples. During sleep, the MINION consumes  $\sim .07$  Watts and roughly 2 Watts for 80 seconds during sampling. If set on an hourly sleep cycle, the batteries would be fully



depleted after about 30 days, however, we reserve about 50% of this power for recovery (burn-wire, strobe and Iridium communications).

### 3.3 Description of the MINION Control System

The following sections provides a detailed description of the Minion platform: electronics, software and operation.

#### 3.3.1 MINION HAT

The MINION HAT (Hardware Attached on Top) PCB evolved over multiple generations resulting in an all-in-one sensor, timing and power management solution for the Raspberry Pi. Similar to the STT camera traps, the on-board ATMEGA328P is programmed to communicate with and power cycle the attached RPi.



(a) MINION HAT Version 2.9 Top



(b) MINION HAT Version 2.9 Bottom

Figure 8: The MINION HAT all in one IO expansion board provides hardware sleep, programmable IO/MOSFETS/LEDs, high accuracy timing, on board sensors and power regulation, all condensed to the form factor of the RPi Zero

Development of the MINION HAT (Figure 8) for multiple uses resulted in the expansion of as much IO as possible for future use. Both the micro-controller and RPi have breakouts for low level serial or interrupt pin actuation. Both processors are also connected to a MOSFET array, 2 controlled by 328 and 4 controlled by RPi. Each channel is capable of 2 Amps of continuous drain for general use i.e. recovery strobe, burn wire. RPi MOSFET 1 on the HAT is used to support the camera illumination as the gate is tied to RPi GPIO 18 (BCM) to send PWM duty cycles for desired brightness.

### **3.3.2 Real Time Clock**

The DS3231 real time clock was chosen for its integrated crystal oscillator, low drift and temperature compensation features. The clock communicates via i2c and is easily enabled as a device tree overlay on the RPi. Time is kept with a 3V CR1220 coin cell battery backup on the HAT.

### **3.3.3 Accelerometer**

Vehicle orientation used to analyze timelapse results is monitored by an on-HAT Analog Devices ADXL345 i2c accelerometer. The 10bit 3 axis device samples at 100 Hz to add another layer of context to sensor readings. In previous experiments this data was used to determine vehicle orientation while sampling.

### **3.3.4 Analog to Digital Converter**

For simple analog to digital conversions on-board, a Texas Instruments ADS1115 i2c ADC is board mounted for creative use-cases. Equipped with 4 single ended or 2 differential inputs this ADC only consumes 150  $\mu$ A in continuous-conversion mode.

### 3.3.5 RPi Camera

The Raspberry Pi Camera Module V2 was demonstrated to be a good tool for marine snow imaging during the 2018 EXPORTS cruise (Section 4.3), and was again chosen for the flux camera. The Sony IMX219 sensor images just above standard 2K resolution (2592 X 1944) using the V4L2 open source driver. The RPi camera is adapted to shoot macro photography by manually unscrewing the included lens from the sensor, about 1.5 rotations, until desired depth of focus is achieved, resulting in high quality macro images for a \$35 camera.

A 12V automotive headlight halo LED ring was determined to provide even and diffused illumination to the imaging surface. While the halo is on, the MINION takes advantage of the RPi's built in white balance and automatic exposure settings to improve imaging performance in the changing lighting conditions of the twilight zone. This comes at the cost of consistent imaging conditions for automated image post-processing, though at this stage imagery is used for qualitative purposes.

### 3.3.6 MS5837-30BA Pressure Sensor

This pressure sensor is sourced from Blue Robotics. Based on the MS5837-30BA sensor by TE Connectivity, the Blue Robotics package comes pre-potted inside a standard Blue Robotics pass-through, thus saving time during assembly. The MS5837-30BA sensor consumes 1.25 mA of current while communicating data via i2c, with a maximum depth reading of 300 meters, reported +/- 200 mbar accuracy and a temperature range of -20 to +85°C the pre-potted device fits the MINION's needs for a low price of \$72. Recently we became aware of a potential drift problem in this sensor during multi-day deployments which will be tested in our ballast tank before we can determine if a replacement sensor is necessary.

### 3.3.7 TSYS01 Temperature Sensor

This \$60 temperature sensor and housing is also sourced from Blue Robotics. Based on the TSYS01 from TE Connectivity it comes in a similar form factor to the Blue Robotics pressure sensor above with the added feature of suspending the potted chip inside an exposed metal cage for increased water flow over the sensor. The sensor consumes 1.4 mA while in use with a temperature range of -40 to +125°C and accuracy of +/- 0.5°C. Though the MS5837 does include a temperature reading to calibrate pressure, this sensor provides higher accuracy for minimal additional investment.

### 3.3.8 Dissolved O<sub>2</sub> Sensor

The incorporation of an optical PreSENS OxyBase WR-RS232 dissolved oxygen sensor further expanded the MINION payload. The OXYbase was chosen for its accuracy and 12mm diameter form factor. The WR-RS232 has a dissolved oxygen detection range between 0 - 22.5 mg/L with accuracy down to 0.01 mg/L. A converter board was made to interface between RPi TTL serial bus and OXYbase RS232 via MAX3232RL. The cost of the sensor at \$1200 significantly adds to the overall cost of the MINION and as such we anticipate not all MINIONs will be equipped with this sensor. As the device name suggests, communication is handled via RS232 through custom TTL to RS232 converter (Figure 9).





(a) Purpose built RS232 to TTL conversion board for OXYbase sensor

(b) OXYbase RS232 Dissolved Oxygen Sensor

Figure 9: The MINION HAT is designed to be adaptable for a wide range of projects and applications.

### 3.3.9 Burn Wire

Upon entering recovery mode, the MINION passes current via MOSFET to the exposed Inconel anode. As current is conducted through the sea water to the cathode, the wire dissolves and the final ballast weight is released. Unlike previous designs, the MINION burn wire design houses all components inside a replaceable pass-through for servicing and redeployment. The burn wire is fed power by the RPi via MOSFET limited by a 30 ohm 5W resistor during the initial stages of recovery until the MINION, informed by the pressure sensor, reaches the surface.

### 3.3.10 Iridium and GPS

In previous iterations of the MINION control system, in order to save money and development cost, a Spot Trace standalone GPS tracker was responsible for relaying the MINION's position for recovery at sea. This off the shelf option left a lot to be desired, between the proprietary device firmware and less than effective internal

antenna, resulting in the exploration of a custom solution (Figure 10).

The integration of a 9602 Iridium modem allows for more resilient location data transmission as well as the capacity to send sensor data to the mainland without the need to recover the MINION. In the case the MINION's resurfacing is delayed or sea state is such that physical recovery of the vehicles is impossible, the MINION is now capable of transmitting the deployment's sensor data via Iridium. Erran Sousa (GSO) developed a standalone GPS+Iridium unit to replace the Spot Trace GPS unit in the previous MINION design.



Figure 10: Iridium 9602, GPS and recovery strobe assembly

### 3.3.11 Reed Switch

The magnetic reed switch located on the MINION endcap controls the enable pin of the system's primary voltage regulator. When the magnet, embedded in the MINION lens cover, is applied the system consumes no power for transit. Removing the magnetic endcap delivers power to the micro-controller and begins the programmed MINION sample cycle. Post recovery, the reed switch is employed to 'wake up' the MINION during sleep cycles by restarting the micro-controller via

power resetting and connecting to the MINION Hub WiFi network

### 3.3.12 Batteries

As with all underwater vehicles, the batteries make up a portion of the total payload weight consideration. 20 LiMnO<sub>2</sub> CR123A 3V batteries by Titanium Innovations (Figure 11) are arranged into a 12V 7 Ah battery pack . The pack is shaped in an open ring and located against the endcap so the traveling weight slide into the center hole keeping the weight as low as possible to maximize float stability during recovery and data transmission.



Figure 11: An off the shelf stack of two CR123a batteries in shrink tube

## 3.4 Software

All software is made publicly available at:

[https://github.com/jacksonsugar/MINION\\_2.9.git](https://github.com/jacksonsugar/MINION_2.9.git)

The repository contains scripts for both the ATMEGA328P and Raspberry Pi as well as installation instructions for both devices.

### 3.4.1 ATMEGA328P

Shared by both the Arduino development boards from previous projects (Section 3.7), the ATMEGA328P satisfies the MINION's needs for a variety of IO as well as low power sleep capabilities. Though the microcontroller is now embedded in



a custom PCB, programming via Arduino IDE is still available for novice programmers. Rather than USB, the microcontroller is programmed via a standalone usbtiny SPI AVR programmer. From the factory, the 328P needs fuses set in order to enable the internal crystal oscillator before the end user uploads the MINION C++ script.

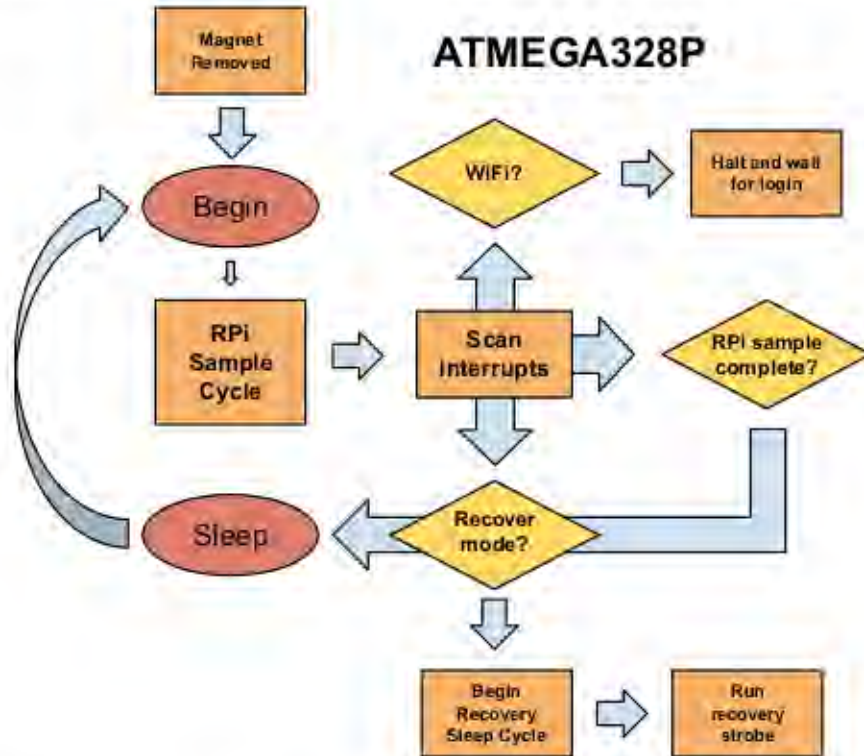


Figure 12: Schematic of the ATMEGA328P flow chart. The microcontroller applies power to the RPi at 'begin'. The RPi sample cycle is described in Figure 5.

Due to the RPi's lack of a power switch or hardware sleep function, the 328P cycles power to the RPi via the enable pin of the secondary 5V power supply. In use, the microcontroller leverages its true hardware sleep function to maintain timing during variable MINION sleep cycles (Figure 12). This allows the MINION to remain idle consuming only 4  $\mu$ Amps of battery power while the main sampling hardware and RPi remain off. The microcontroller receives simple digital inputs



from the RPi via GPIO in order to determine the computer's power state and receive recovery signals. While active and sampling, the RPi communicates its intention to continue processing until the intended script is complete. Once the MINION completes its final sample cycle, or if the mission is aborted, the RPi will instruct the 328P to begin the recovery procedure.

### 3.4.2 Raspberry Pi Zero W

Programming the Raspberry Pi is a different experience compared to the 328P as it is a fully featured Linux computer. All MINION software is written in Python for consistency. The MINION\_2.9 github repository includes an automated installation script with simple questions to configure IP address and data storage location of each MINION. After the installation process, the MINION is contactable via ssh, the RTC is configured and up to date and all drivers/sampling scripts are updated and stored within `/Documents/`. Communication with the MINIONS going forward takes place in `MINION_config.ini` within the end user's custom data directory. Editing the config file below allows the end user to change many of the basic mission parameters (Figure 13).

## MINION CONFIG FILE

```

* # Mission Stats, Reset to 0 if
* triggered, Max_Depth in meters
* [Mission]
* Abort = 0
* Max_Depth = 300
*
* # Initial pressure and temperature
* readings. Camera sample rate in
* minutes. Sensor sample rate in Hz.
* [Initial_Samples]
* hours = .05
* Camera_sample_rate = 10
* TempPres_sample_rate = 5
* Oxygen_sample_rate = 1
*
* # Post wire burn data collection
* time. Camera sample rate in
* minutes. Sensor sample rate in Hz.
* [Final_Samples]
* hours = .05
* Camera_sample_rate = 10
* TempPres_sample_rate = 5
* Oxygen_sample_rate = 1
*
* # Time elapsed from deployment to
* ballast drop.
* [Deployment_Time]
* days = 0
* hours = 10
*
* # Sleep cycle programmed on
* microcontroller in hours.
* [Sleep_cycle]
* Minion_sleep_cycle = .25
*
* # Sensor sample rate (Hz) and time (min.)
* per power cycle.
* # If sample time same as Camera time
* sample_time = Camera
* # Suggested Oxygen sample rate <= 1 Hz
* [Data_Sample]
* Minion_sample_time = Camera
* Minion_sample_rate = 5
* Oxygen_sample_rate = 1
*
* # Sampling methods
* [Sampling_scripts]
* Image = True
* TempPres = True
* Temperature = True
* Oxybase = False
* ACC_100Hz = False

```

Figure 13: An example of the MINION RPi Config file.

The MINIONDeploymentHandler.py and all sampling scripts reference the config file for tracking mission progress and sample rate instructions.

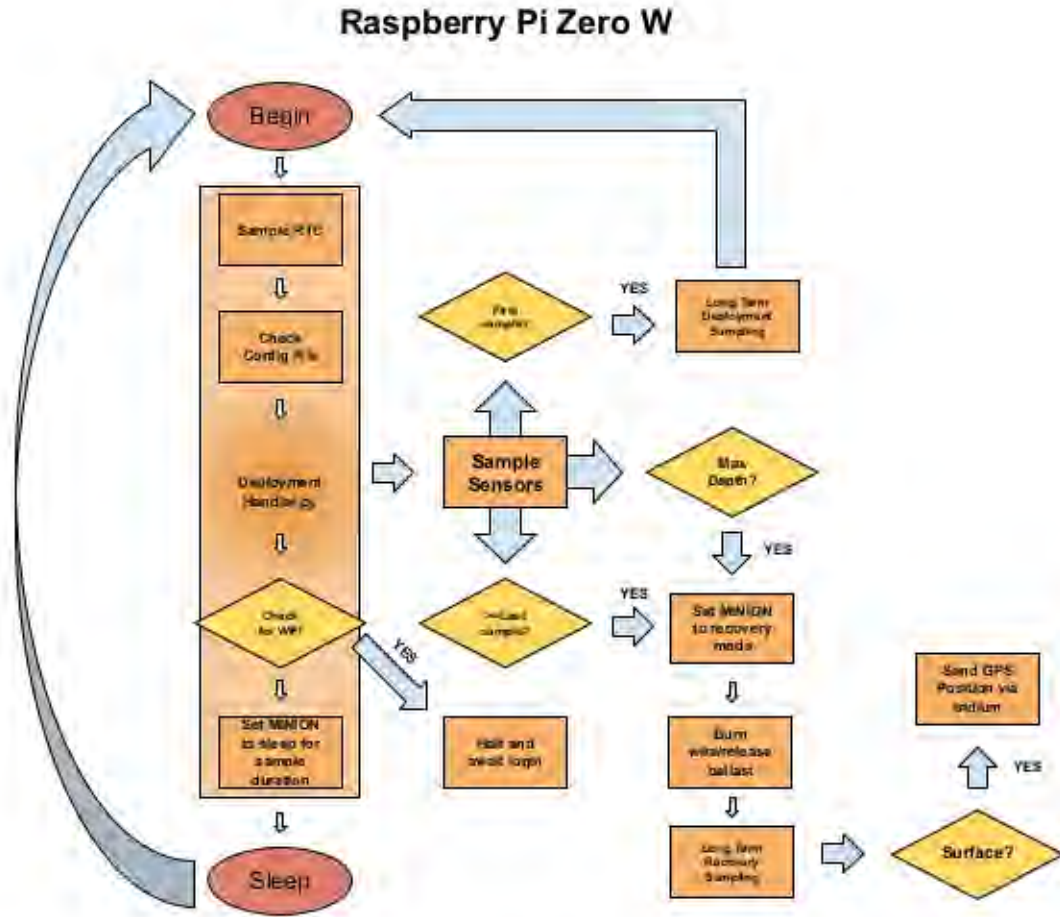


Figure 14: MINION RPi Software Flow Chart

During deployment, the MINION\_DeploymentHandler script (Figure 14) keeps track of its progress by monitoring the number of time lapse image samples collected. Acting like a service daemon, the DeploymentHandler is responsible for updating the RTC file, scan for WiFi during sample cycles and relay power state information to the ATMEGA328P. Before enclosing electronics, the MINION sleep cycle duration is programmed to the ATMEGA328P micro-controller via usbtiny serial programmer.

To configure all MINION behaviors other than sleep cycle duration, the user supplies the included WiFi access point with power and removes the magnetic lens

cap from the MINION. The user then connects their laptop to the MINION\_Hub access point and ssh (Secure SHell) login to the on board computer. Navigating to and editing `/Desktop/MINION_config.ini` via WiFi gives the end user flexibility in sampling all in one place. Before deployment the end user is to ensure all data directories are clear of files and ensure MINION\_Hub WiFi is unplugged. WiFi is the only method used to program, configure and retrieve data off of the float.

### 3.5 Deployment

To deploy, remove magnetic lens cap and wait for the red LED on the HAT to trigger to ensure the MINION correctly began initial sampling. Once sampling, lower device into ocean and release. We found that a simple slip line with release pin (Figure 15) worked well while operating off a larger vessel.



Figure 15: MINION being lowered off the stern of the R/V Sally Ride SR1919

At the beginning of the MINION Life Cycle (Fig. 6, A), the Pi checks the data

output directory for samples, if none are present it will sample all sensors for the configured initial sample time to track the MINION's descent to its target isopycnal. Once complete, the MINION begins the sleep cycle.

The MINION will continue to cycle power and sample for the configured mission duration (Fig. 6, C & D).

During the mission, while the RPi is active, the pressure sensor is sampled continuously in case the MINION surpasses its configured maximum operating depth. In such case, the MINION will abort mission and begin recovery procedures early.

### **3.6 Recovery**

After the last time lapse photo is taken, the Pi communicates to the 328P to begin recovery. The RPi releases the ballast and the MINION samples all sensors continuously while ascending to the surface. The RPi, informed by the pressure sensor, ensures the MINION reaches the surface before attempting to send location and sensor data via Iridium (Fig. 6, F). Due to the small size of the MINIONs, fish net style recovery from the side of larger research vessels can be performed safely (Figure 16).





Figure 16: MINION recovery during SR1919 cruise

After recovery, the end user powers on the provided WiFi access point and power cycles the MINION using the magnetic safety cap. The RPi will boot up and inform the microcontroller it is connected to WiFi and remain powered. This allows the user full access to the MINION to recover data and configure future deployments remotely via ssh. The end user then can shut down the Pi and reinstall the safety cap to save the on board batteries.

### 3.7 MINION Precursors

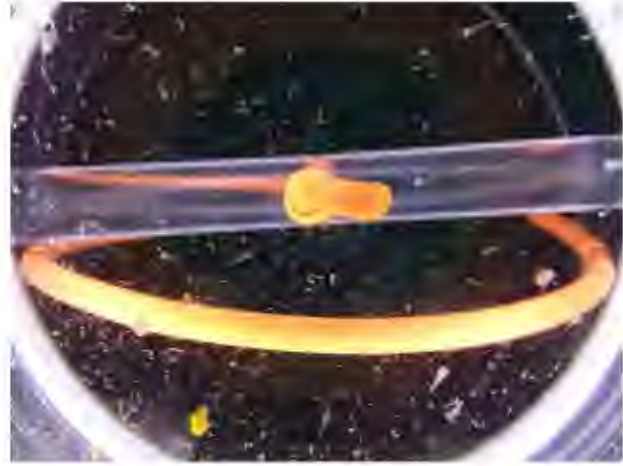
Before completion of the first Minion prototype, various pre-cursors enabled me to demonstrate and refine discrete aspects of the design. The following sections describe some of these activities I completed while I was an undergraduate working in Dr. Omand's lab.

### 3.7.1 Surface Tethered Trap (STT) Timelapse Gel Cameras

The STT (Surface Tether Trap) gel cameras were developed as a means to evaluate the suitability of the Raspberry Pi Foundation's Camera Module 2.0 for imaging marine snow particles (Figure 17a). These camera units were mounted beneath a traditional cylindrical particle-intercepting trap with a 15cm diameter. The base of the trap contained a cup with a polyacrylimide gel layer that trapped and preserved the particles once they arrived at the base. The bottom of the cup and the upper face of the camera housing were transparent, allowing us to collect a timelapse sequence of the arrival of particles over a series of 8 day deployments (Figure 17b). This was the first system that used a microcontroller (Arduino Pro Mini) to act as a low power programmable timing solution for the Raspberry Pi Zero W. The low power sleep features of the microcontroller (2  $\mu$ Amps) proved to be a key feature, allowing us to obtain a long timelapse sequence with minimal battery usage. The three units initially built successfully collected hundreds of photos at 15 minute intervals during nine, eight day long deployments (Section 4.3). The cameras were mounted on the top three frames of the surface-tethered array, at 100m, 150m and 200m depth. Upward-looking images with 2K resolution appeared to be effective at resolving the color, size and shape of most marine snow aggregates and zooplankton fecal pellets - the two most important contributors to sinking carbon flux (Smith et al. 2018).[1]



(a) STT gel cameras on the bench during the cruise



(b) An example of an Image captured by STT gel camera. The photo illustrates the size range and quality of particle images that can be obtained with this system, generally encompassing marine snow aggregates, fecal pellets, swimmers, and smaller particles that range from 500  $\mu\text{m}$  to 1 cm.

Figure 17: Surface Tethered Trap Gel camera examples from NASA EXPORTS 2018

### 3.7.2 Burn-Wire Strobe units

Initially, we had planned to use a self-contained, timed, load-bearing release mechanism (BWS) for the MINIONs, and so we developed a prototype in early 2017, initially using breakouts and later with a custom printed circuit board (PCB). The internals - including a Arduino Nano (later ATMEGA328P on PCB version), a real-time clock, batteries, strobe and burnwire - were potted into a 1" OD acrylic tube (Figure 18). One end was sealed with the burnwire parts, and the other end was left open for communication via a mini USB (later female headers). It became clear fairly early on that the BW design would preclude accurate float ballasting, since we would need to seal the unit in order to ballast and then would be un-



able to change mission details as needed, as so it was abandoned as a MINION component.

However, the BWS became an essential recovery aid for the APEX-NBST (Neutrally Buoyant Sediment Trap) during EXPORTS 2018 and we worked to fulfill a large demand for these in advance of that cruise. To date, we have built more than 120 of these devices for testing and field use. The basic operation is as follows: An off the shelf development board (Nano or ATMEGA328P chip on PCB) is programmed to wake at a predetermined elapsed or real-time. It stays asleep ( $2\ \mu\text{Amps}$ ) checking the real-time clock every 4 seconds. At wake up, power is episodically supplied to the strobe, and an electric current is delivered to a nickel alloy wire loop that holds the ballast weight (or trap lids as is the case for the NBSTs). The wire corrodes and the weight is released, allowing the float to rise to the surface (or the lids to close). The development and extensive testing and field deployment of these units significantly improved our understanding of the anode/cathode solution of the release mechanism that was later incorporated into the MINION housing. Incorporation of the BWS units onto the NBSTs is described in Estapa et al. 2019. [2]



Figure 18: Internals of the self contained burn wire to be potted in an acrylic tube

## List of References

- [1] K. L. Smith, H. A. Ruhl, C. L. Huffard, M. Messié, and M. Kahru, "Episodic organic carbon fluxes from surface ocean to abyssal depths during long-term monitoring in NE Pacific," *Proceedings of the National Academy of Sciences*, vol. 115, no. 48, pp. 12235–12240, 2018. [Online]. Available: <https://www.pnas.org/content/115/48/12235>
- [2] M. Estapa, J. Valdes, K. Tradd, J. Sugar, M. Omand, and K. Buesseler, "The neutrally buoyant sediment trap: two decades of progress," *Journal of Atmospheric and Oceanic Technology*, vol. 0, no. 0, p. null, 2019. [Online]. Available: <https://doi.org/10.1175/JTECH-D-19-0118.1>

## CHAPTER 4

### Results from Research Cruises

The following sections briefly describes cruises that enabled demonstration of the MINION or MINION precursors.

#### 4.1 EN601

In the summer of 2017 the R/V Endeavor set sail in the Gulf of Mexico with the intention of validating a small form factor hydrophone/recorder for tracking of small fish and lobsters[1]. These recorders, named Fish Tags (Section 5.1.1), were confirmed capable to suitably resolve sub-surface geolocation greater than 60 Km from the sound sources with an error between 70 and 560 meters [2]. Figure 19 details the experimental data collected during testing. Employing this underwater tracking solution for MINIONs will help constrain the trajectory of the vehicles underwater post recovery. Integration of these tags is planned, but not as part of this thesis.

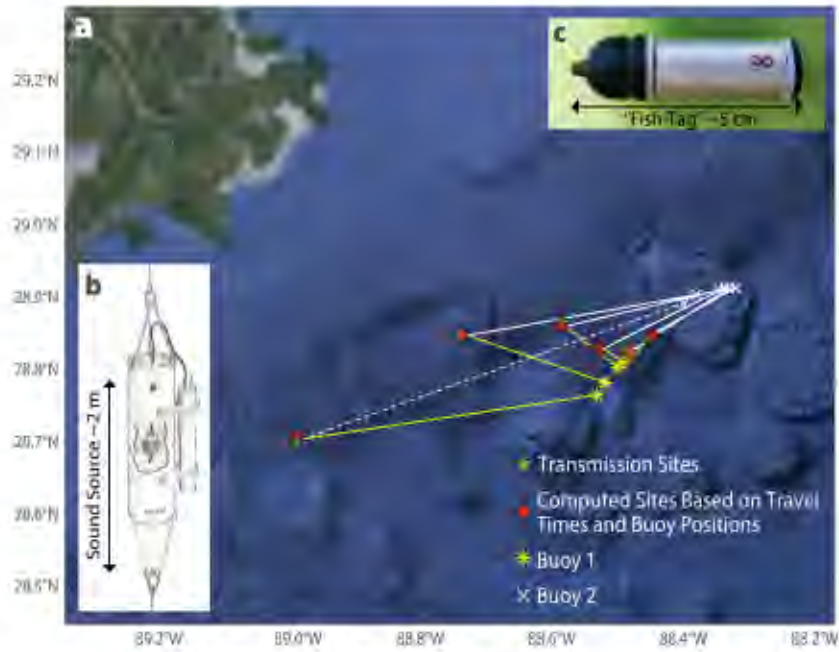


Figure 19: Results from Fish Tag test in the Gulf of Mexico confirming accurate localization of deployed tags. Figure reproduced from Rossby et al. 2017

## 4.2 EN610

In preparation for EXPORTS 2018 the R/V Endeavor was employed to test deployments of the Neutrally Buoyant Sediment Traps (NBSTs) [3] with burn wire integration (Figure 20). The NBST consists of four sediment trap tubes mounted around an APEX float for Lagrangian sampling of carbon flux. The trap tubes are held open by an elastic bungee secured to the self contained burn wire unit. Before the APEX float is scheduled to resurface, the burn wire release closes the sediment trap tubes to ensure all particles are recovered. During the trip, burn wires were attached to a deep sea lander and demonstrated functionality at depths in excess of 4000 meters.

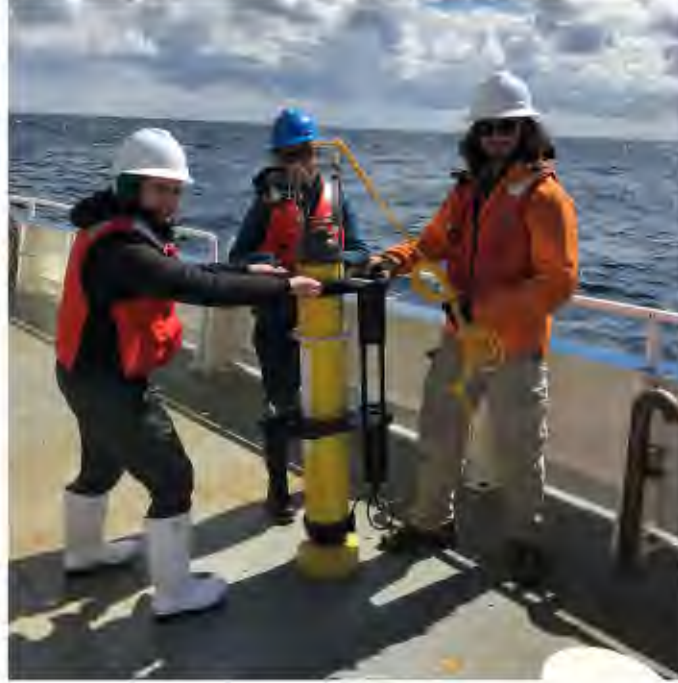


Figure 20: NBST Recovery with burn wire attached and sediment trap tubes removed from SOLO float

### 4.3 NASA EXPORTS 2018

The first mass deployments of NBSTs and deployments of the Surface Tethered Trap (STT) gel cameras occurred during the summer of 2018. The STT cameras yielded high resolution time lapses of descending carbon snow within the twilight zone (Figure 21). The image data we collected informed our decision to continue using the Raspberry Pi Foundation Camera Module V2.1, as the fixed focal distance produced good quality images for a very low hardware cost.

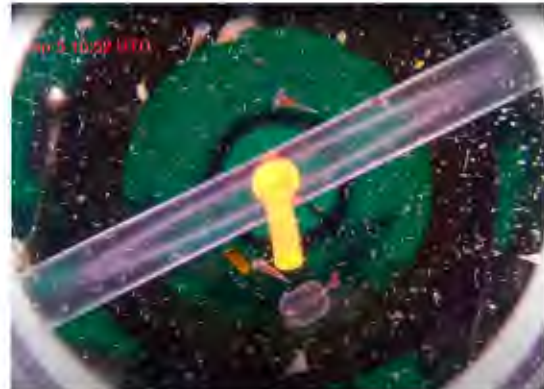


Figure 21: Surface Tethered Trap gel camera time lapse image



#### 4.4 SR1919

This trip marked the first opportunity to deploy fully functional MINIONs at sea. During the winter of 2019, I joined on a cruise led by Dr. Alyson Santoro aboard the R/V Sally Ride. Three MINIONs were deployed off the southern California coastline for 12 h missions. The goal was to verify the vehicle's capability of completing the entire mission cycle, and gain experience with deployment and recovery.

The first MINION deployment (Minion 101) was quite discouraging as it did not sink as we intended. This was later attributed to the lack of a sufficient early release ballast weight. With a last minute innovation from one of the SR's res-techs we fashioned a slip mechanism that held the MINION more firmly in the water before release (Figure 22).



Figure 22: Removing magnetic image surface cover during MINION deployment

The last two MINIONs successfully sank (Figure 23) with 30 grams of additional temporary weight (held by a pre-dissolved fruit flavor life saver candy) that allowed the MINION to break through the warm surface mixed layer. With fairly calm sea state and clear skies we had no trouble recovering these two MINIONs after 24 hours. Figure 23 shows the pressure data from both MINION 102 and 103 (top panel). These two were both ballasted to hit an isopycnal around 45 meters. Minion 102 did land at this depth though it was likely a fluke. Minion 103 went deeper - to about 140m, so we have some refinements to make to our ballasting

method. Regardless, since both of them settled on an isopycnal, took photos and measurements and were recovered, these deployments were considered a success. The pressure records provided valuable insights into the descent rate of the floats. A closer look at Minion 102's approach reveals an initial descent at about 6 m/s (Fig. 23 lower panel). After a couple of minutes, the lifesaver dissolved and dropped the extra ballast. The Minion then rose and toward its neutral density. We can then see it move up and down with internal waves of about 5 minute period. A more detailed analysis of this behavior, and an analysis of vehicle properties like drag, is planned for a future paper.

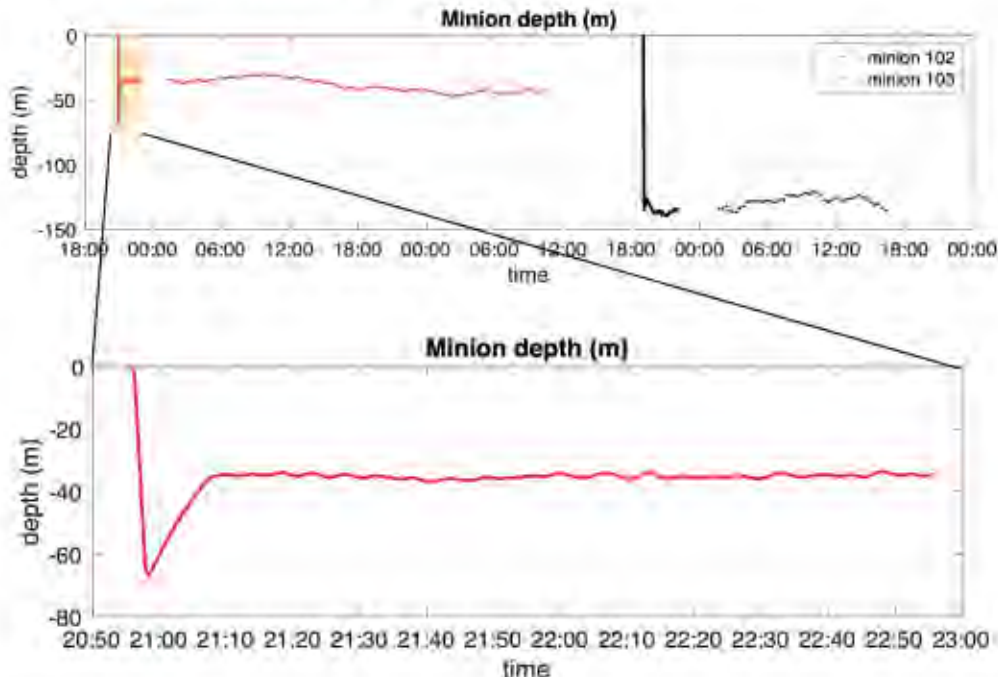


Figure 23: MINION pressure data from SR1919. Top panel shows the entire two records. Bottom panel shows a zoomed in view of the first 2 hours of MINION 102.

#### 4.5 AR43

Armstrong43 was the first cruise opportunity to deploy MINIONs rough, open ocean conditions in early March 2020. The plan dictated deployment of two MINIONs in the same location with a deployment time of 5 days and 12 hours before



retrieval. Just before deployment, a surface drifter was launched in order to compare the MINIONs' subsurface trajectory with a surface float. The MINIONs were programmed to begin recovery procedures 18 hours ahead of schedule to ensure they surfaced by the scheduled recovery time. On the day of recovery the MINIONs failed to report back and the Armstrong returned home.

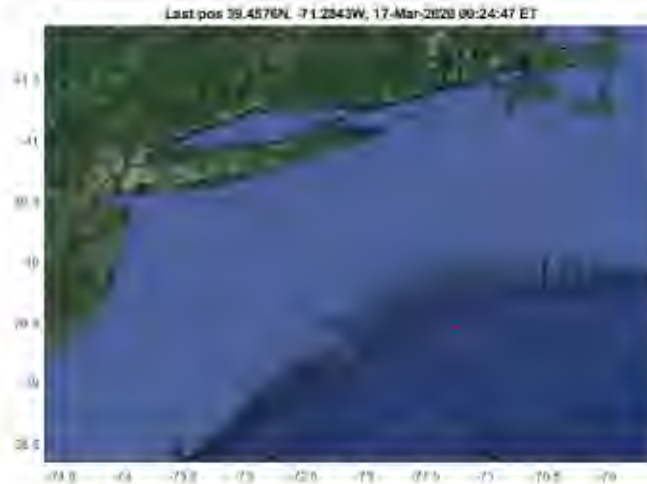


Figure 24: Comparison of surface drifter and MINION track after one week with same deployment site. The dashed red track represents the surface drifter, the red dots are MINION GPS transmissions with the green X marks the final GPS call.

The next evening MINION 102 began to show activity. The MINION continued to drift for the next 9 hours before issuing a low battery warning and ultimately going dark (Figure 24). We concluded the MINIONs had trouble calling in because of the wavy conditions and the fairly small distance the float extended out of the water. We hope that a more robust satellite communication solution will be found with the 9602 Iridium modem and longer tubes.

## List of References

- [1] G. Fischer, T. Rossby, and D. Moonan, "A Miniature Acoustic Device for Tracking Small Marine Animals or Submerged Drifters," *Journal of Atmospheric and Oceanic Technology*, vol. 34, no. 12, pp. 2601–2612, 12 2017. [Online]. Available: <https://doi.org/10.1175/JTECH-D-17-0127.1>

- [2] T. Rossby, G. Fischer, and M. Omand. "A New Technology for Continuous Long-Range Tracking of Fish and Lobster," *Oceanography*, vol. 30, no. 2, June 2017. [Online]. Available: <https://doi.org/10.5670/oceanog.2017.217>
- [3] M. Estapa, J. Valdes, K. Tradd, J. Sugar, M. Omand, and K. Buesseler.

## CHAPTER 5

### Conclusion

#### 5.1 Future Development

There are numerous developments planned for the next generation of floats that go beyond the scope of this thesis. For the MINIONs to reach the goal of becoming expendable, acoustic tracking, extended battery life, on-board image processing, and a scuttling function will be integrated. These upgrades are briefly outlined below:

##### 5.1.1 Acoustic tags

A miniature multipurpose acoustic tag developed at URI by Godi Fisher, Tom Rossby and Daniel Moonan, known as the fish tag [1] was designed with mid water drifters in mind. Potted within the hydrophone exterior, the self contained unit houses accurate timing, pressure sensor, temperature sensor, signal processing and on board memory to support standalone acoustic tracking based on RAFOS triangulation.

Integration of these acoustic tags would allow for geolocalization while the MINIONs are underway (though not in real-time) (Figure 18). As the MINIONs are Lagrangian, this mid-water location data will help place MINION measurements into a spatial context. Dr. Omand is working with URI professor Dr. Godi Fischer and Dr. Tom Rossby to supply these for the MINION.

##### 5.1.2 LiSOC12 Lithium Batteries

One of the simplest ways to increase longevity of the MINIONs is through increasing battery capacity. Though the unit cost per cell doubles, the LiSOC12 (lithium

thionyl chloride (LTC)) AA form-factor battery (Figure 25) chemistry delivers 8.64 Wh per cell over the previous 4.8 Wh per cell offering massive gains in deployment time.



Figure 25: Single 3.6V LTC AA Battery by Xeno Energy

Unlike traditional batteries where voltage measurement is a good indication of discharge level, the LTC battery maintains output voltage until almost 10% power remains. This is beneficial to ensure ample power delivery to Iridium hardware during data recovery at the end of the mission.

In order to monitor the new battery supply, an i2c Texas Instruments BQ35100 will be embedded on the battery pack for coulomb counting during deployment. During operation, the RPi resets the counter after new batteries are installed and can receive warning when the batteries approach total depletion.

### 5.1.3 Expendable MINION Features

As MINIONS are deployed in larger quantities and for longer time spans it becomes less feasible to physically recover the vehicles for data analysis. Opposed to the current recovery protocol, transmitting location for retrieval, the expendable MINION will process both sensor and image data for Iridium transmission. The Raspberry Pi on board computer is compatible with many source image quan-

tification/classification software packages for pre-transmission image processing i.e. OpenCV, TensorFlow or other Linux compatible software. Once data transmission is complete, the expendable MINION's final mission is to sink to avoid becoming floating debris. Methods to reliably sink the vehicle post data transmission are still being discussed.

## 5.2 Conclusion

The MINION platform demonstrates the viability of employing low cost hardware and power saving strategies to collect dispersed, long term data sets for measurements in the ocean twilight zone. The control system can be configured to sample for days to months at a time. Autonomous, with failure modes in place to recover itself in the event of a malfunction. The platforms are much smaller and cheaper to produce than previous sampling methods allowing ease of shipping and en-masse deployments. Sampling and telemetry is handled by a flexible Linux single board computer for future sensor inclusion and upgrades, with programming made simple via WiFi configuration. The first large scale deployment (up to 20 MINIONs) was scheduled for May of 2020 during the 2020 NASA EXPORTS cruise (Canceled due to Covid-19). We look forward to evaluating the performance of the most recent revision of the MINION during the rescheduled 2021 cruise.

## List of References

- [1] G. Fischer, T. Rossby, and D. Mooney, "A Miniature Acoustic Device for Tracking Small Marine Animals or Submerged Drifters," *Journal of Atmospheric and Oceanic Technology*, vol. 34, no. 12, pp. 2601–2612, 12 2017. [Online]. Available: <https://doi.org/10.1175/JTECH-D-17-0127.1>



## BIBLIOGRAPHY

- Bishop, J. K. B., Fong, M. B., and Wood, T. J., "Robotic Observations of High Wintertime Carbon Export in California Coastal Waters," *Biogeosciences*, vol. 13, no. 10, pp. 3109–3129, 2016. [Online]. Available: <https://bg.copernicus.org/articles/13/3109/2016/>
- Bower, A. S., "Potential Vorticity Balances and Horizontal Divergence along Particle Trajectories in Gulf Stream Meanders East of Cape Hatteras," *Journal of Physical Oceanography*, vol. 19, no. 11, pp. 1669–1681, 01 Nov. 1989. [Online]. Available: [https://journals.ametsoc.org/view/journals/phoc/19/11/1520-0485\\_1989\\_019\\_1669\\_pvbahd.2.0.co;2.xml](https://journals.ametsoc.org/view/journals/phoc/19/11/1520-0485_1989_019_1669_pvbahd.2.0.co;2.xml)
- Buesseler, K. "Pump it Up Workshop Report." [Online]. Available: <https://hdl.handle.net/1912/9328>
- Estapa, M., Valdes, J., Tradd, K., Sugar, J., Omand, M., and Buesseler, K., "The neutrally buoyant sediment trap: two decades of progress," *Journal of Atmospheric and Oceanic Technology*, vol. 0, no. 0, p. null, 2019. [Online]. Available: <https://doi.org/10.1175/JTECH-D-19-0118.1>
- Fischer, G., Rossby, T., and Moonan, D., "A Miniature Acoustic Device for Tracking Small Marine Animals or Submerged Drifters," *Journal of Atmospheric and Oceanic Technology*, vol. 34, no. 12, pp. 2601–2612, 12 2017. [Online]. Available: <https://doi.org/10.1175/JTECH-D-17-0127.1>
- Rommich, D., Sherman, J. T., Davis, R. E., Grindley, K., McClune, M., Parker, C. J., Black, D. N., Zilberman, N., Purkey, S. G., Sutton, P. J. H., and Gilson, J., "Deep SOLO: A Full-Depth Profiling Float for the Argo Program," *Journal of Atmospheric and Oceanic Technology*, vol. 36, no. 10, pp. 1967–1981, 01 Oct. 2019. [Online]. Available: <https://journals.ametsoc.org/view/journals/atot/36/10/jtech-d-19-0066.1.xml>
- Rossby, Dorson, and Fontaine, "The RAFOS System," *Journal of Atmospheric and Oceanic Technology*, vol. 3, no. 4, pp. 672–679, 1986. [Online]. Available: [https://doi.org/10.1175/1520-0426\(1986\)003<0672:TRS>2.0.CO;2](https://doi.org/10.1175/1520-0426(1986)003<0672:TRS>2.0.CO;2)
- Rossby, T., Fischer, G., and Omand, M., "A New Technology for Continuous Long-Range Tracking of Fish and Lobster," *Oceanography*, vol. 30, no. 2, June 2017. [Online]. Available: <https://doi.org/10.5670/oceanog.2017.217>

Smith, K. L., Ruhl, H. A., Huffard, C. L., Messic, M., and Kahru, M.,  
“Episodic organic carbon fluxes from surface ocean to abyssal depths during  
long-term monitoring in NE Pacific,” *Proceedings of the National Academy  
of Sciences*, vol. 115, no. 48, pp. 12 235–12 240, 2018. [Online]. Available:  
<https://www.pnas.org/content/115/48/12235>